Inorg. Chem. **1982**, *21*, 1383–1387 **1383**

Contribution from the Department of Chemistry,
University of Calgary, Calgary, Alberta, Canada T2N 1N4

Synthesis, Structure, and Temperature-Dependent ^{1}H NMR Spectra of Tetraphenylarsonium μ-Chloro-bis(μ-isobutylthiolato)-bis(dichlorooxotungstate(V))

VIKRAM D. PATEL,[1] P. MICHAEL BOORMAN,* K. ANN KERR, and KELLY J. MOYNIHAN

Received June 25, 1981

The new complex $[Ph_4As]^+[Cl_2OW(\mu\text{-}Cl)(\mu\text{-}S\text{-}i\text{-}Bu)_2WOCl_2]^-$ has been structurally characterized by a single-crystal X-ray structural determination. Crystals are monoclinic, space group $P2_1/n$, with $Z = 4$ in a cell of dimensions $a = 11.440$ (3) Å, $b = 17.421$ (3) Å, $c = 18.932$ (5) Å, and $\beta = 90.03$ (1)°. Intensity data were collected on an automated diffractometer at −100 (5) °C and were used for a full-matrix least-squares refinement on F, which converged at $R_1 = 0.042$. The structure is confacial bioctahedral with the oxo ligands cis to one another. Variable-temperature ^{1}H NMR in CD_2Cl_2 and $C_2D_2Cl_4$ show that two isomers exist in solution at room temperature that differ in the configuration of the μ-S-*i*-Bu groups. With use of the coalescence temperature, an activation energy of 72 ± 5 kJ mol^{-1} for inversion at the μ-S atoms was obtained.

Introduction

The coordination chemistry of tungsten shows many similarities to that of its lighter congener, molybdenum. In the 5$^+$ oxidation state, the chemistry of molybdenum is dominated by the molybdenum–oxygen bond.[2,3] However, in contrast to the large variety of well-characterized oxomolybdenum(V) species containing the structural units[2-7] $[MoO]^{3+}$ (A, B) $[Mo_2O_3]^{4+}$ (C), and $[Mo_2O_4]^{2+}$ (D) (Figure 1), relatively few oxotungsten(V) complexes have been reported.[8] Of the known oxotungsten(V) species, by far the largest number are monomeric (structural type A). The paucity of data on binuclear oxotungsten(V) species was highlighted by the recent syntheses and structural characterizations of $[W_2O_4(EDTA)]^{2-}$[9,10] and $[W_2O_4F_6]^{4-}$.[11] These complexes were the first examples of the general class which contain $[W_2O_4]^{2+}$ units (type D). To date, however, binuclear tungsten complexes of types B and C have not been reported.

While attempting to extend our earlier work on synthetic routes to tungsten thiolate clusters (eq 1, $n = 1$,[12] $n = 2$[13]),

$$WCl_4L_2 + nMe_3SiSR \rightarrow [WCl_{4-n}(SR)_nL_2] + nMe_3SiCl$$

$$[WCl_{4-n}(SR)_nL_2] \xrightarrow[\text{degradation}]{\text{spontaneous}} \text{products} \qquad (1)$$

$$L = Me_2S,\ C_4H_8S;\ R = Et,\ i\text{-}Bu$$

we allowed $WCl_4(SMe_2)_2$ to react with 3 molar equiv of (isobutylthio)trimethylsilane. The objective was to synthesize polynuclear tungsten thiolate clusters by reductive elimination of R_2S_2 from the $[WCl_{4-n}(SR)_nL_2]$ intermediate as previously observed.[13] However, during attempts to crystallize pure products by derivatizing the crude mixture in the presence of Ph_4AsCl, the solution was allowed to evaporate slowly in the presence of air. The red crystalline product so isolated proved to be $[Ph_4As]^+[W_2O_2Cl_4(\mu\text{-}Cl)(\mu\text{-}S\text{-}i\text{-}Bu)_2]^-$ (**1**). Herein we report the characterization of this compound by a single-crystal X-ray structural determination and the solution behavior of the complex as determined by ^{1}H NMR spectroscopy over a range of temperatures. The characterization of this complex confirms the expectation that triply bridged oxotungsten(V) dimeric complexes can be prepared. It is the first member of this class to be reported.[29]

Experimental Section

General Procedures. The adduct $WCl_4(Me_2S)_2$ was prepared by direct reaction of WCl_4 and the ligand, as previously described.[14] Isobutylthiotrimethylsilane was synthesised from the lead salt of *i*-BuSH by the published procedure.[15] The handling of $WCl_4(Me_2S)_2$ and $Me_3Si(S\text{-}i\text{-}Bu)$ was carried out in an atmosphere of pure, dry nitrogen. Solvents were dried over CaH_2 or P_4O_{10} and were distilled and degassed before use. $Ph_4As^+Cl^-$ was obtained as the hydrate from Alfa Products and was dehydrated by heating under vacuum for 16 h at 100 °C.

Synthesis. $[Ph_4As]^+[W_2O_2Cl_5(S\text{-}i\text{-}Bu)_2]^-$ was prepared serendipitously by the following procedure. $WCl_4(Me_2S)_2$ (1.03 g, 2.29 mmol) was dissolved in CH_2Cl_2 (ca. 30 mL), and to this stirred solution was added $Me_3SiS\text{-}i\text{-}Bu$ (3 molar equiv), also dissolved in CH_2Cl_2 (ca. 2 mL of solution). The color changed immediately from light red to dark red, which deepened to brown after stirring for 15 h. The solution was then pumped down to an oil to remove solvent and volatile byproducts (Me_3SiCl, $i\text{-}Bu_2S_2$, Me_2S). The oil was redissolved in CH_2Cl_2 (50 mL), and to this solution was added Ph_4AsCl (0.99 g, 2.2 mmol). After 15 h of stirring under N_2, no crystalline product had appeared. The solution was therefore allowed to evaporate slowly in air, whereupon well-formed crystals of the title compound were deposited. Elemental analysis and IR spectra suggested that the compound had the formula $[Ph_4As]^+[W_2O_2Cl_5(i\text{-}BuS)_2]^-$. Anal. Calcd for $W_2Cl_5C_{32}H_{38}S_2O_2As$: C, 33.75; H, 3.34; As, 6.58; Cl, 15.57 W, 32.31. Found: C, 34.00; H, 3.40; As, 6.50; Cl, 15.5; W, 31.1%. IR data (2000–200 cm^{-1}) obtained from a Nujol mull between CsI plates: (270 w, 300 vs, 335 vs, 345 m, and 360 s assigned to ν(W–Cl)), 455 m, 460 vs, 480 s, 690 vs, 780 w, 790 vs, 845 m (930 w, 960 s, and 980 vs assigned to ν(W=O)), 1000 s, 1080 s, 1163 m, 1180 m, 1240 w cm^{-1}. The UV–visible spectrum was recorded on a CH_2Cl_2 solution with a Cary 219 spectrophotometer (wavelength in nm; extinction coefficient (ϵ) in parentheses): 427 (469); 351 sh (2945); 306 (6810). ^{1}H NMR data (200 MHz) are discussed below. The variable-temperature spectra were recorded with a Varian XL-200 FT-NMR spectrometer, equipped with a variable-temperature device, and the measured temperatures are considered accurate to ±1 °C.

Collection and Reduction of X-ray Data. The compound $[Ph_4As]^+[W_2O_2Cl_5(i\text{-}BuS)_2]$, prepared as above, crystallized from CH_2Cl_2 solutions as needles, almost square in cross section. The sample chosen for data collection (0.24 × 0.12 × 0.11 mm) was obtained

---

(1) Abstracted in part from a thesis submitted to the University of Calgary by Vikram D. Patel in partial fulfillment of the requirements for the Ph.D. degree.

(2) Stiefel, E. I. *Prog. Inorg. Chem.* **1977**, *22*, 1 and references therein.

(3) Spivack, B.; Dori. Z. *Coord. Chem. Rev.* **1975**, *17*, 99.

(4) Boyd, I. W.; Dance, I. G.; Landers, A. E.; Wedd, A. G. *Inorg. Chem.* **1979**, *18*, 1875.

(5) Swedo, K. B.; Enemark, J. H. *J. Chem. Educ.* **1979**, *56*, 70.

(6) Huneke, J. T.; Yamanouchi, K.; Enemark, J. H. *Inorg. Chem.* **1978**, *17*, 3695.

(7) Yamanouchi, K.; Enemark, J. H. *Inorg. Chem.* **1978**, *18*, 1626.

(8) Dori, Z. *Prog. Inorg. Chem.* **1981**, *28*, 239.

(9) Khalil, S.; Sheldrick, B.; Soares, A. B.; Sykes, A. G. *Inorg. Chim. Acta* **1977**, *25*, L83.

(10) Khalil, S.; Sheldrick, B. *Acta Crystallogr., Sect. B* **1978**, *B34*, 3751.

(11) von Mattes, R.; Mennemann, K. *Z. Anorg. Allg. Chem.* **1977**, *437*, 175.

(12) Boorman, P. M.; Kerr, K. A.; Patel, V. D. *J. Chem. Soc., Dalton Trans.* **1981**, 506.

(13) Boorman, P. M.; Patel, V. D.; Kerr, K. A.; Codding, P. W.; Van Roey, P. *Inorg. Chem.* **1980**, *19*, 3508.

(14) (a) Boorman, P. M.; Chivers, T.; Mahadev, K. N. *Can. J. Chem.* **1975**, *53*, 383. (b) Schaefer-King, M. A.; McCarley, R. E. *Inorg. Chem.* **1973**, *12*, 1972.

(15) Abel, E. W. *J. Chem. Soc.* **1960**, 4406.

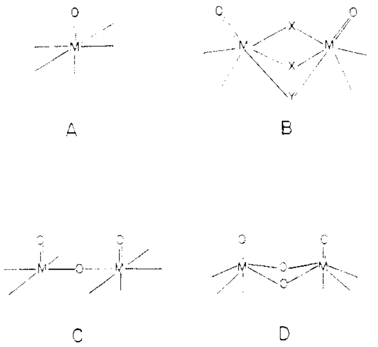

Figure 1. Some known structures of oxomolybdenum(V) complexes.

by cutting a larger crystal transverse to the needle axis. It was mounted on a glass fiber in epoxy resin and was also lightly coated with the resin to prevent possible aerial degradation during the data collection. The crystal was then mounted in an arbitrary orientation on an Enraf-Nonius CAD-4 automatic diffractometer fitted with a Universal low-temperature device. After the crystal was centered, the Enraf-Nonius program SEARCH was used to obtain 25 accurately centered reflections which were then employed to obtain an orientation matrix via the program INDEX. The program TRANS identified a monoclinic cell, which was verified by comparison of equivalent reflections in a small data set ($\theta < 10°$) covering an entire sphere of reflections. The space group was then identified as $P2_1/n$ from the systematic absences for $0k0$, $k = 2n + 1$, and for $h0l$, $h + l = 2n + 1$. The E statistics later confirmed the centrosymmetric space group. Cell constants and an orientation matrix were then determined by a least-squares refinement of the setting angles of 25 reflections with high θ values. The crystal was then cooled to −100 (5) °C, and the centering procedures were repeated to obtain the low-temperature cell constants and orientation matrix. Data were collected in the $\omega/2\theta$ scan mode with a scan width of $\Delta\omega = 1.5(0.6 + 0.35 \tan \theta)°$. Of the 6876 independent reflections measured in the range $2° \leq \theta \leq 25°$, 1839 had intensity greater than $3\sigma(I)$ where $\sigma(I) = (P + 4B)^{1/2}$, P is the sum of the counts accumulated in the central 64 steps of the scan, and B is the sum of the counts in the 16 steps at either end of the scan. Most reflections were measured with a scan speed of $(20/3)°$ min^{-1}, but weak reflections were measured at speeds as low as $(20/40)°$ min^{-1} to improve counting statistics. Two standard reflections ($5\bar{1}1$, $\bar{6}41$) were measured every 1000 s of exposure. The data were normalized by the program DATCO5 to compensate for a small (6%) systematic decrease in intensity over the course of the data collection. Standard Lorentz and polarization corrections were applied as was an absorption correction with use of the program CADABS[16] (μ = 78.3 cm^{-1}). Seven crystal faces were identified: 010, $0\bar{1}0$, 001, $00\bar{1}$, $\bar{1}00$, $1\bar{1}0$, and 101. The minimum and maximum values of the correction were 2.20 and 2.47, respectively.

Table I. Crystal Data

molecular formula	$(C_{24}H_{30}As)^+[W_2O_2Cl_5S_2C_8H_{18}]^-$			
mol wt	1138.6			
crystal system	monoclinic			
space group	$P2_1/n$			
cell constants				
a, Å	11.533 (3)	21 °C	11.440 (3)	−100 °C
b, Å	17.623 (5)		17.421 (3)	
c, Å	19.133 (4)		18.932 (5)	
β, deg	90.05 (4)		90.03 (1)	
V, Å^3	3888 (2)		3773 (1)	
medium for density measmt (flotation)	$CCl_4/CHBr_3$			
density (obsd, 21 °C), g cm^{-3}	1.93			
density (calcd, 21 °C), g cm^{-3}	1.94			
Z	4			
symmetry constraints	none			
μ, cm^{-1}	78.3			
radiation	Mo Kα (graphite monochromator), λ = 0.710 69 Å			
max θ	25°			

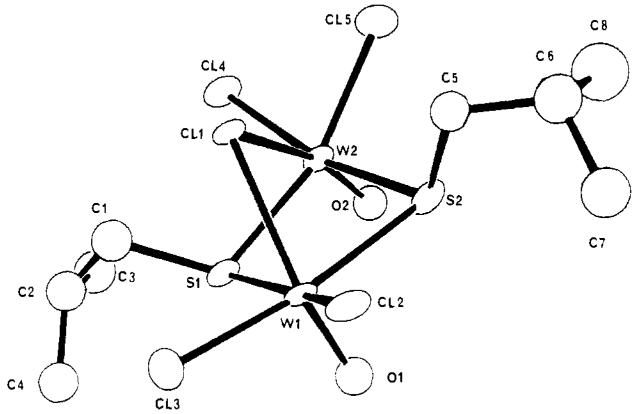

Figure 2. ORTEP view of the anion in the complex $[Ph_4As]^+[W_2O_2Cl_4(\mu\text{-}Cl)(\mu\text{-}S\text{-}i\text{-}Bu)_2]^-$ displaying the thermal ellipsoids at 50% probability and showing the atom numbering scheme.

Solution and Refinement of the Structure. The structure was solved by the heavy-atom method and refined by full-matrix least-squares techniques on F. The scattering factors were taken from Cromer and Mann[17] and the anomalous dispersion corrections from ref 18. The refinement proceeded smoothly, with anisotropic thermal parameters for the heavy atoms and isotropic thermal parameters for the carbon atoms. The phenyl groups were refined as rigid groups, and phenyl hydrogen atoms were included in the model in the final refinement cycles but were not refined. Secondary extinction could not be refined successfully and was therefore not included. The maximum shift to error ratio in the final cycle was 0.000 83, with the average value 0.000 12. An electron density difference map revealed no peaks of chemical significance, but several peaks occurred within 1 Å of the tungsten atoms with heights of up to 0.15 e Å^{-3}. The weighting scheme used was $w = [1.2\sigma^2(F) + 0.0025F^2]^{-1}$. Statistical analysis of the average value of $w\Delta^2(F)$ over ranges of $|F_o|$ and $(\sin \theta)/\lambda$ showed no systematic trends. The final R values are $R_1 = \sum||F_o| - |F_c||/\sum|F_o|$ = 0.042 for 1839 contributing reflections, and $R_2 = [\sum w(|F_o| - |F_c|)^2/\sum w(F_o)^2]^{1/2} = 0.052$. The standard deviation of an observation of unit weight was 0.896.

The final positions of the nonhydrogen atoms are given in Table II, with atoms labeled according to Figure 2. A listing of the positions of the phenyl carbon atoms, the calculated positions of the phenyl hydrogen atoms, and the observed and calculated structure factor amplitudes and the $\sigma(F)$ values is available as supplementary material.

The XRAY-76 programs[19] were used for all calculations, unless otherwise stated.

Results and Discussion

The structure (Figure 2) of the $[W_2O_2Cl_5(S\text{-}i\text{-}Bu)_2]^-$ anion could be described as confacial bioctahedral, with Cl$^-$ and two i-BuS$^-$ groups occupying the bridging positions. The trans labilizing influence of the oxo groups can be observed in the relatively long bonds from W(1) and W(2) to Cl(1) (Table III). The structure could alternatively be described as an edge-share bis(square-pyramidal) structure, with a sixth more distant ligand (Cl(1)) approximately trans to the two oxo ligands.[4] Analysis of the structure by least-squares planes calculations (Table VI) shows that the metal–ligand atom skeleton has approximate C_{2v} symmetry. This, of course, is not crystallographically required. The inclusion of the isobutyl groups would remove any vestige of this symmetry. The obtuse angle between the W(1)S(1)S(2) and W(2)S(1)S(2) planes is 205.6°, which describes the folding of the molecule along

---

(16) CADABS, a local modification of a program by P. Coppens to calculate absorption factors by numerical Gaussian integration: *Acta Crystallogr.* **1965**, *18*, 1035.

(17) Cromer, D. T.; Mann, J. B. *Acta Crystallogr., Sect. A* **1968**, *A24*, 321.

(18) "International Tables for X-ray Crystallography"; Kynoch Press: Brimingham, England, 1974.

(19) Technical Report TR-446; Stewart, J. M., Ed.; Computer Science Centre, University of Maryland.

Table II. Positional and Thermal Parameters[a] and Their Estimated Standard Deviations for $[Ph_4As]^+[W_2O_2Cl_4(\mu\text{-Cl})(\mu\text{-S-}i\text{-Bu})_2]^-$

atom	x	y	z	U_{11}	U_{22}	U_{33}	U_{12}	U_{13}	U_{23}
W(1)	0.2185 (1)	0.17871 (7)	0.14221 (7)	1.26 (6)	2.67 (8)	3.31 (9)	−0.48 (6)	−0.86 (6)	−0.15 (8)
W(2)	0.0280 (1)	0.22994 (7)	0.05688 (7)	1.80 (6)	2.08 (7)	2.70 (8)	−0.33 (7)	−0.98 (6)	0.72 (8)
As	0.3476 (2)	0.4297 (2)	0.8962 (1)	1.4 (1)	1.4 (2)	2.7 (2)	−0.4 (1)	−1.0 (1)	−0.0 (1)
Cl(1)	0.0106 (5)	0.1133 (4)	0.1427 (4)	1.3 (3)	2.5 (4)	3.1 (5)	−0.4 (3)	−1.1 (3)	0.1 (3)
Cl(2)	0.2322 (6)	0.1686 (5)	0.2672 (4)	2.0 (4)	4.2 (5)	3.7 (5)	−0.5 (4)	−1.4 (3)	−0.1 (4)
Cl(3)	0.3124 (7)	0.0576 (5)	0.1462 (5)	4.1 (5)	3.2 (5)	7.0 (7)	1.2 (4)	−2.4 (5)	−1.5 (5)
Cl(4)	−0.0810 (6)	0.1656 (5)	−0.0318 (4)	2.4 (4)	4.4 (6)	4.0 (5)	−0.6 (4)	−1.8 (4)	0.2 (4)
Cl(5)	−0.1596 (6)	0.2726 (5)	0.0915 (4)	2.5 (4)	4.0 (5)	4.0 (5)	0.3 (4)	−0.8 (3)	1.3 (5)
S(1)	0.1881 (6)	0.1494 (4)	0.0189 (4)	2.1 (4)	2.9 (5)	3.1 (5)	−0.8 (3)	−0.6 (4)	0.1 (4)
S(2)	0.0913 (6)	0.2863 (4)	0.1676 (4)	2.9 (4)	1.8 (5)	4.3 (5)	−0.8 (4)	−0.9 (4)	0.7 (4)

atom	x	y	z	U, Å^2	atom	x	y	z	U, Å^2
O(1)	0.328 (2)	0.239 (1)	0.119 (1)	3.6 (5)	C(4)	0.654 (2)	−0.007 (2)	0.050 (2)	3.5 (8)
O(2)	0.083 (2)	0.302 (1)	0.012 (1)	3.4 (5)	C(5)	−0.007 (2)	0.269 (2)	0.242 (1)	3.2 (7)
C(1)	0.145 (2)	0.046 (2)	0.000 (1)	2.8 (8)	C(6)	−0.018 (3)	0.344 (2)	0.283 (2)	4.6 (9)
C(2)	0.212 (3)	0.018 (2)	−0.063 (2)	4.3 (9)	C(7)	0.101 (3)	0.368 (2)	0.315 (2)	4.9 (10)
C(3)	0.686 (3)	0.437 (2)	0.368 (2)	5.4 (10)	C(8)	−0.070 (3)	0.415 (2)	0.239 (2)	6.0 (11)

[a] The corresponding data for the phenyl carbon and hydrogen atoms are available as supplementary Tables 1 and 2, respectively.

Table III. Bond Distances (Å) with Estimated Standard Deviations in Parentheses for the Anion $[W_2O_2Cl_4(\mu\text{-Cl})(\mu\text{-S-}i\text{-Bu})_2]^-$

W(1)–W(2)	2.854 (2)		
W(1)–Cl(1)	2.635 (6)	W(2)–Cl(1)	2.609 (7)
W(1)–Cl(2)	2.378 (8)	W(2)–Cl(4)	2.372 (8)
W(1)–Cl(3)	2.368 (8)	W(2)–Cl(5)	2.363 (7)
W(1)–O(1)	1.69 (2)	W(2)–O(2)	1.64 (2)
W(1)–S(1)	2.414 (8)	W(2)–S(1)	2.416 (7)
W(1)–S(2)	2.421 (7)	W(2)–S(2)	2.425 (8)
S(1)–C(1)	1.89 (3)	S(2)–C(5)	1.82 (3)
C(1)–C(2)	1.50 (4)	C(5)–C(6)	1.53 (4)
C(2)–C(3)	1.56 (5)	C(6)–C(7)	1.55 (5)
C(2)–C(4)	1.56 (4)	C(6)–C(8)	1.61 (5)

Table IV. Bond Angles (Deg)

	W–Bridge–W Angles		
W(1)–Cl(1)–W(2)	66.0 (2)		
W(1)–S(2)–W(2)	72.2 (2)	W(1)–S(1)–W(2)	72.4 (2)
	Bridge–W–Bridge Angles		
Cl(1)–W(1)–S(1)	77.5 (2)	Cl(1)–W(2)–S(1)	77.9 (2)
Cl(1)–W(1)–S(2)	78.0 (2)	Cl(1)–W(2)–S(2)	78.4 (2)
S(1)–W(1)–S(2)	105.6 (3)	S(1)–W(2)–S(2)	105.4 (2)
	Bridge–W–Terminal Angles		
Cl(1)–W(1)–O(1)	159.4 (6)	Cl(1)–W(2)–O(2)	161.1 (7)
Cl(1)–W(1)–Cl(2)	91.3 (2)	Cl(1)–W(2)–Cl(4)	91.9 (2)
Cl(1)–W(1)–Cl(3)	91.3 (2)	Cl(1)–W(2)–Cl(5)	90.2 (2)
S(1)–W(1)–O(1)	89.0 (7)	S(1)–W(2)–O(2)	90.0 (7)
S(1)–W(1)–Cl(2)	162.9 (3)	S(1)–W(2)–Cl(5)	162.4 (3)
S(1)–W(1)–Cl(3)	84.7 (3)	S(1)–W(2)–Cl(4)	85.0 (2)
S(2)–W(1)–O(1)	91.1 (7)	S(2)–W(2)–O(2)	91.1 (7)
S(2)–W(1)–Cl(2)	84.2 (3)	S(2)–W(2)–Cl(5)	84.4 (2)
S(2)–W(1)–Cl(3)	162.9 (3)	S(2)–W(2)–Cl(4)	163.7 (2)
	Terminal–W–Terminal Angles		
Cl(2)–W(1)–O(1)	105.0 (7)	Cl(5)–W(2)–O(2)	104.5 (7)
Cl(2)–W(1)–Cl(3)	82.7 (3)	Cl(4)–W(2)–Cl(5)	82.4 (2)
Cl(3)–W(1)–O(1)	102.9 (7)	Cl(4)–W(2)–O(2)	101.6 (7)
	Carbon–Sulfur–Metal Angles		
C(1)–S(1)–W(1)	114.7 (9)	C(5)–S(2)–W(1)	113.3 (10)
C(1)–S(1)–W(2)	114.2 (9)	C(5)–S(2)–W(2)	114.4 (9)

Table V. Nonbonded Distances (Å)

Cl(1)···S(1)	3.16 (1)	Cl(1)···Cl(2)	3.59 (1)
Cl(1)···S(2)	3.19 (1)	Cl(1)···Cl(3)	3.58 (1)
S(1)···S(2)	3.85 (1)	Cl(1)···Cl(4)	3.58 (1)
O(1)···O(2)	3.62 (3)	Cl(1)···Cl(5)	3.52 (1)
S(1)···O(1)	2.92 (2)	S(1)···Cl(4)	3.23 (1)
S(1)···O(2)	2.92 (2)	S(1)···Cl(3)	3.22 (1)
S(2)···O(1)	2.98 (2)	S(2)···Cl(2)	3.22 (1)
S(2)···O(2)	2.95 (2)	S(2)···Cl(5)	3.22 (1)
Cl(2)···Cl(3)	3.13 (1)	Cl(4)···Cl(5)	3.12 (1)
Cl(2)···O(1)	3.26 (2)	Cl(4)···O(2)	3.14 (2)
Cl(3)···O(1)	3.20 (2)	Cl(5)···O(2)	3.19 (2)

Table VI

Least-Squares Plane Calculations

plane	atoms in plane	σ (plane)	dist of atoms from plane, Å
1	W(1), S(1), S(2)	0.000	
2	W(2), S(1), S(2)	0.000	
3	S(1), S(2), Cl(1), Cl(2)	0.005	W(1), 0.263
4	S(1), S(2), Cl(3), Cl(4)	0.027	W(2), 0.257
5	O(1), W(1), Cl(1), W(2), O(2)	0.013	Cl(2), 1.593; Cl(3), −1.542; Cl(5), 1.555; Cl(4), −1.563; S(1), −1.906; S(2), 1.946
6	S(1), Cl(1), S(2)	0.000	Cl(2), 2.949; Cl(3), 2.958; O(1), 1.79; W(1), 1.428; W(2), −1.426; O(2), −1.83; Cl(4), −2.966; Cl(5), −2.914

Angles between planes

planes	angle	planes	angle
1, 2	205.6	5, 6	90.2
3, 4	226.1		

the S···S vector. An alternative way of considering this is via the obtuse angle between the two square planes Cl(2)Cl(3)-S(1)S(2) and Cl(4)Cl(5)S(1)S(2), which is 226.1°. The W atoms are displaced from these square planes by 0.26 Å, toward the oxo ligands. There is no strong structural evidence to suggest that a W–W bond exists. The W···W distance (2.854 (2) Å) is slightly longer than that reported[20] for $[W_2(\mu\text{-S})_2(Et_2NCS_2)_2(MeO)_4]$ (2.791 Å) in which a W–W single bond has been assigned. However, attempts to use the criteria of Cotton and Ucko[21] for assigning M–M bonding in confacial bioctahedral structures lead to ambiguity. For example, the angles subtended at the bridging sulfur (W–S–W = 72.3 (2)°) are consistent with an almost pure bioctahedron, with no displacement of the metals toward each other. The W(1)–Cl(1)–W(2) angle (66.0 (2)°) would suggest the converse, but as mentioned above the W–Cl distances are abnormally long, which inevitably would result in a reduction of the W–Cl–W angle. The other point of interest in this structure in the configurational geometry of the bridging

---

(20) Bino, A.; Cotton, F. A.; Dori, Z.; Sekutowski, J. C. *Inorg. Chem.* **1978**, *17*, 2946.

(21) Cotton, F. A.; Ucko, D. *Inorg. Chim. Acta* **1972**, *6*, 161.

Table VII. Comparison of the Geometry of $[W_2O_2Cl_4(\mu\text{-}Cl)(\mu\text{-}S\text{-}i\text{-}Bu)_2]^-$ (**1**) and $[Mo_2O_2(\mu\text{-}SPh)_2(\mu\text{-}Cl)(S_2CNEt_2)_2]^+$ (**2**)

	1[a]	**2**[b]
M–M, Å	2.854 (2)	2.822 (2)
$(M-Cl_{br})_{av}$	2.622 (8)	2.613 (12)
$(M-O)_{av}$	1.66 (2)	1.656 (6)
$(M-S_{br})_{av}$	2.418 (8)	2.457 (8)
$(M-S-M)_{av}$, deg	72.3 (2)	70.09 (7)
M–Cl–M, deg	66.0 (2)	65.35 (7)
$O-M-Cl_{br}$, deg	160.2 (3)	158.2 (2)
$O-M-S_{br}$, deg	90.0 (7)	95.6 (1)
$[S_{br}-M(1)-S_{br}][S_{br}-M(2)-S_{br}]$, deg	205.6	182.3
sum of angles subtended at bridging S (av), deg	300.6	285.6
terminal atom–metal–terminal atom (av),[c] deg	82.5 (3)	72.2 (1)
C–S–M, deg	114.1	107.8

[a] This work. [b] Reference 22. [c] Cl–W–Cl in **1**; S_t-Mo-S_t in **2**.

thiolates. The alkyl groups both lie in equatorial positions, giving an ee isomer. As discussed below, the solution properties suggest that another isomer can readily exist.

Molybdenum complexes similar to the $[W_2O_2Cl_5(S\text{-}i\text{-}Bu)_2]^-$ ion (**1**) have been reported by Enemark[22] and Wedd[4] and their co-workers. The cation **2** contains a triply bridged oxo-molybdenum(V) moiety as shown.[22] The terminal ligands are diethyldithiocarbamate species, rather than Cl^- ions as contained in **1**. The important structural parameters of **1** and **2** are compared in Table VII. This table shows that the two structures are remarkably similar. However, the chelating dithiocarbamate ligands in **2** constrain the S_t-Mo-S_t bond angles to a value 10° lower than the corresponding Cl_t-W-Cl_t angles in **1**. The second notable difference lies in the sum of the angles subtended at the bridging thiolato sulfur atoms. The acute $M-S_{br}-M$ angles (70 ± 2°) are similar in both complexes, but the angles involving carbon are greater in **1**, implying a closer approach to planarity of the thiolate sulfur in this system. This may be related to the fluxional behavior discussed later. The $M(S_{br})_2M$ fragment in **2** is almost planar whereas in **1** there is significant folding. Comparisons with similar molybdenum complexes are given in ref 4 and 6 and will not be repeated here.

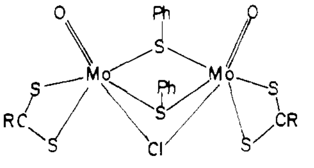

2, R = Et_2N

^{1}H NMR Studies. The anion **1** is capable of existence as the isomers I–III as shown (viewed down the W···W axis). The isomers arise from the possible configurations of the μ-thiolato groups. As shown, in the solid state the ee (III) isomeric form is adopted.

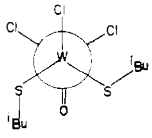

I

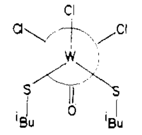

II

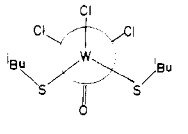

III

In solutions in CD_2Cl_2 and $C_2D_2Cl_4$, two isomers exist as revealed by the ^{1}H NMR spectra. The spectra, taken at 200 MHz, are temperature dependent (Figure 3), indicating a dynamic equilibrium between the two isomers.

In the slow-exchange region (35 °C), three well-resolved doublets are observed for the methylene protons of the isobutyl groups (δ 3.66, 3.43, and 3.26), with the resonances at δ 3.66 and 3.26 being of equal intensity. However, the corresponding methyl (δ 1.12–1.16) and methyne (δ 2.38–2.56) resonances are not as well resolved. The CH_2 proton resonances indicate the presence of two isomers in the slow-exchange limit: the unsymmetrical (ae) isomer I (δ 3.66, 3.26) and one of the symmetrical isomers II (aa) or III (ee) (δ 3.43). In view of the observed solid-state structure possessing the ee configuration, this is the probable symmetrical structure, which is partially retained upon dissolution of the complex. Although the complex **2**, discussed above, exhibits an aa solid-state configuration of the thiolate groups,[22] the ability of the phenyl substituents to lie parallel to each other would minimize the steric repulsions normally expected of this arrangement.[23] Such interactions would be expected to be large for the relatively bulky isobutyl groups. We therefore assign the symmetric isomer in solution as the ee isomer (III). The ratio of concentrations of ee:ae obtained from integration of the methylene resonances is ca. 2:1. When the temperature is raised, the CH_2 resonances coalesce to a broad singlet (75–85 °C). Similar but less well-resolved effects occur for the CH_3 and CH protons. The CH_2 resonance continues to sharpen until, at 125 °C, a well-resolved doublet is observed. These spectral changes are completely reversible and are interpreted as being the consequence of rapid interconversion between ae $\rightleftharpoons$ ee isomers at the fast-exchange limit (125 °C) (see inset, Figure 3).

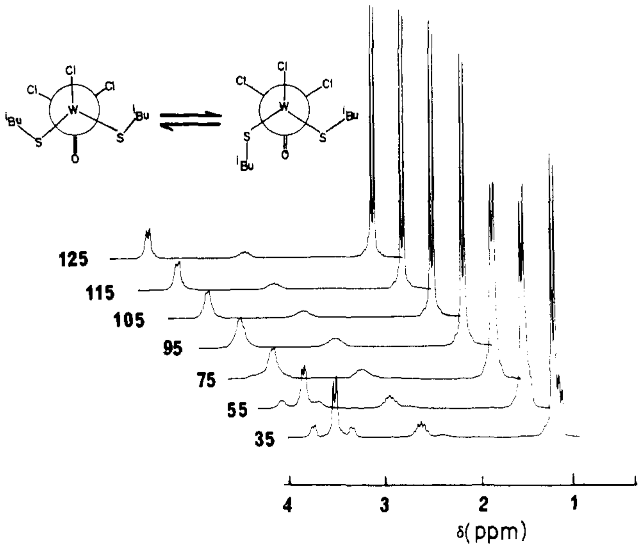

Figure 3. 200-MHz variable-temperature (°C) ^{1}H NMR spectrum of $[Ph_4As]^+[W_2O_2Cl_4(\mu\text{-}Cl)(\mu\text{-}S\text{-}i\text{-}Bu)_2]^-$ in $C_2D_2Cl_4$ (isobutyl region shown). The scale refers to the spectrum at 35 °C. The spectra at higher temperatures are offset by 60 Hz with respect to the lower temperature spectra.

Application of the following equation[24] yields a free energy of activation ΔG = 75 ± 5 kJ mol^{-1}:

$$\Delta G = -RT_c \ln \left[\frac{2\pi h(\Delta\nu)}{kT_c\{3[1 + 3^{1/2}(p_A - p_B)]\}^{1/2}} \right] \quad (2)$$

where $\Delta\nu$ = separation of resonances of the two isomers in the slow-exchange limit ($\Delta\nu$ = 36 ± 1 Hz), T_c = coalescence temperature (363 ± 5 K), and p_A, p_B are fractional populations of isomers A and B (0.66 for ee; 0.33 for ae). Other symbols have their usual significance.

---

[22] Bunzey, G.; Enemark, J. H.; Gelder, J. I.; Yamanouchi, K. *J. Less-Common Met.* **1977**, *54*, 101.

[23] Dahl, L. F.; Wei, C. H. *Inorg. Chem.* **1963**, *2*, 328.

[24] Lynden-Bell, R. M. *Prog. Nucl. Magn. Reson. Spectrosc.* **1967**, *2*, 181.

Comparison with data published for analogous complexes shows that the averaging process at the high-temperature limit may be attributed to inversion at the tricoordinate sulfur atoms: $[Fe_2(CO)_5L(\mu\text{-S-}t\text{-Bu})_2]_2$,[25] L = CO, ΔG = 77 kJ mol^{-1} and L = Ph_3P, ΔG = 66 kJ mol^{-1}; *trans*-$[Ru(CO)(\mu\text{-}SCH_2Ph)(C_5H_5)]_2$,[26] ΔG = 58.7 kJ mol^{-1}. For these complexes the inversion barriers may be correlated with the angles subtended at the bridging sulfur. Thus in strongly metal–metal-bonded structures, the very acute M–S–M angles appear to impede inversion as expected if the process requires a trigonal-planar transition state at sulfur.[27] So that this hypothesis could be tested, the complex $W_2Cl_4(\mu\text{-S-}i\text{-Bu})_2(\mu\text{-}S)(SMe_2)_2]$[28] has been synthesized. It is isoelectronic and isostructural with $W_2Cl_4\ (\mu\text{-SEt})_2(\mu\text{-S})(C_4H_8S)_2$ for which the W—S(Et)—W bond angles are ca. 62°, due to the short W=W bond.[12] For this complex, which differs from **1** in the smaller W–S–W angle, one would predict a higher barrier to inversion at sulfur. Consistent with this prediction, only one isomer can be detected in solution over the accessible range of temperatures.

Acknowledgment. We thank the Natural Sciences and Engineering Research Council of Canada for financial support. The assistance of Dr. R. Yamdagni in obtaining NMR spectra and helpful discussions with Dr. E. A. Dixon are gratefully acknowledged.

Registry No. 1, 80288-48-8; $WCl_4(Me_2S)_2$, 53922-82-0.

Supplementary Material Available: A listing of observed and calculated structure factors and $\sigma(F)$ values and Tables S1 and S2 containing the coordinates of the phenyl carbon and hydrogen atoms, respectively (28 pages). Ordering information is given on any current masthead page.

---

(25) Natile, G.; Maresca, L.; Bor, G. *Inorg. Chim. Acta* **1977**, *23*, 37.

(26) Killops, S. D.; Knox, S. A. R. *J. Chem. Soc., Dalton Trans.* **1978**, 1260.

(27) (a) Turley, P. C.; Haake, P. *J. Am. Chem. Soc.* **1967**, *89*, 4617. (b) Abel, E. W.; Farrow, G. W.; Orrell, K. G.; Sik, V. *J. Chem. Soc., Dalton Trans.* **1977**, 42.

(28) Boorman, P. M.; Patel, V. D., unpublished results.

(29) Since the submission of this article, two papers on the syntheses and redox properties of binuclear tungsten complexes of type B have appeared: (a) Hanson, G. R.; Brunette, A. A.; McDonell, A. C.; Murray, K. S.; Wedd, A. G. *J. Am. Chem. Soc.* **1981**, *103*, 1953. (b) Bradbury, J. R.; Masters, A. F.; McDonell, A. C.; Brunette, A. A.; Bond, A. M.; Wedd, A. G. *Ibid.* **1981**, *103*, 1959.

Contribution from the Department of Chemistry, Faculty of Science, Hiroshima University, Hiroshima 730, Japan,
and Research Laboratories, Fujisawa Pharmaceutical Company, Ltd., Kashima-2-chome, Yodogawaku, Osaka 532, Japan

Structural and Kinetic Trans Influence in (Amino acidato)cobalt(III) Complexes? α-Hydrogen Exchange and Crystal and Molecular Structure of *mer*-Tris(glycinato)cobalt(III) Dihydrate

AKIYOSHI MIYANAGA,[1a] USHIO SAKAGUCHI,[1a] YUKIYOSHI MORIMOTO,[1b] YOSHIHIKO KUSHI,[1a]
and HAYAMI YONEDA*[1a]

Received December 24, 1980

The rate of the α-hydrogen-exchange reaction of glycinato ligands in *mer*-tris(glycinato)cobalt(III) has been found to be different for the three stereochemically different glycinato ligands. This rate difference is interpreted as resulting from the trans influence; the carboxyl oxygen ligand is more effective than the amino nitrogen ligand in labilizing the trans α-hydrogen. The relevance of the trans influence to the α-hydrogen-exchange reaction has been tested and seems to be substantiated for several (glycinato)cobalt(III) chelates. To see if the above reactivity difference is reflected in the molecular structure, we performed the single-crystal X-ray analysis of *mer*-$[Co(H_2NCH_2CO_2)_3]\cdot 2H_2O$ to R_F = 0.047 and R_{wF} = 0.062 for 2101 reflections with $|F| > 3[\sigma(|F|)]$. The crystal is orthorhombic, $Pna2_1$, with a = 15.331 (2) Å, b = 13.205 (2) Å, c = 11.606 (2) Å, and Z = 8. The three glycinato ligands are coordinated in the meridional geometry to complete a nearly octahedral cobalt center. The Co–N bond trans to oxygen is shortened relative to the average length of mutually trans Co–N bonds by 0.022 (3) Å. This structural feature correlates with the rate data, and it seems probable that the kinetic trans influence as found for the α-hydrogen-exchange reaction results, at least partially, from the structural trans influence.

The activation of α-hydrogens of amino acids[2] and peptides[3] through coordination to metal ions has been studied by several workers. The works in this area have been reviewed recently by Pasini and Casella.[4] Previously, we have found,[5] and recently Norman and Phipps[6] confirmed, that the exchange reaction of the α-hydrogens of three stereochemically different glycinato ligands in *mer*-tris(glycinato)cobalt(III), *mer*-$[Co(gly)_3]$, proceeds at unequal rates. At that time we could give no explanation to it nor an assignment to the proton NMR spectrum of this compound in deuterium oxide. Similarly, as we will show here, Norman and Phipps could not make a correct assignment.

On the other hand, we have subsequently shown that the chemical shift of α-hydrogens of amino acids and α-aminocarboxylates coordinated to cobalt(III) can be explained quantitatively, in the absence of valence angle distortion, by the effect of the magnetic anisotropy of the central cobalt ion.[7]

---

(1) (a) Hiroshima University. (b) Fujisawa Pharmaceutical Co., Ltd.

(2) (a) Williams, D. H.; Busch, D. H. *J. Am. Chem. Soc.* **1965**, *87*, 4644. (b) Buckingham, D. A.; Marzilli, L. G.; Sargeson, A. M. *Ibid.* **1967**, *89*, 5133. (c) Gillard, R. D.; Laurie, S. H.; Price, D. C.; Phipps, D. A.; Weick, C. F. *J. Chem. Soc., Dalton Trans.* **1974**, 1385. (d) Dabrowiak, J. C.; Cooke, D. W. *Inorg. Chem.* **1975**, *14*, 1305. (e) Golding, B. T.; Gainsford, G. J.; Herlt, A. J.; Sargeson, A. M. *Tetrahedron* **1976**, *32*, 389. (f) McClarin, J. A.; Dressel, L. A.; Legg, J. I. *J. Am. Chem. Soc.* **1976**, *98*, 4150. (g) Gillard, R. D.; O'Brien, P.; Norma, P. R.; Phipps, D. A. *J. Chem. Soc., Dalton Trans.* **1977**, 1988. (h) Dempsey, A.; Phipps, D. A. *Inorg. Chim. Acta* **1979**, *36*, L425.

(3) (a) Gillard, R. D.; Mitchell, P. R.; Payne, N. C. *Chem. Commun.* **1968**, 1150. (b) Gillard, R. D.; Phipps, D. A.; *J. Chem. Soc. D* **1970**, 800. (c) Browning, I. G.; Gillard, R. D.; Lyons, J. R.; Mitchell, P. R.; Phipps, D. A. *J. Chem. Soc., Dalton Trans.* **1972**, 1815.

(4) Pasini, A.; Casella, L. *J. Inorg. Nucl. Chem.* **1974**, *36*, 2133.

(5) Yoneda, H.; Morimoto, Y. *Proc. Symp. Coord. Chem., 17th* **1967**, 126.

(6) Norman, P. R.; Phipps, D. A. *Inorg. Chim. Acta* **1977**, *24*, L35.

0020-1669/82/1321-1387$01.25/0